Mathematical Biosciences and Engineering

MBE, 19(3): 3056–3068.
DOI: 10.3934/mbe.2022141
Received: 02 November 2021
Revised: 18 December 2021
Accepted: 28 December 2021
Published: 19 January 2022

http://www.aimspress.com/journal/MBE

Research article

Wavelets and digital filters designed and synthesized in the time and frequency domains

Viliam Ďuriš[1,*], Vladimir I. Semenov[2] and Sergey G. Chumarov[3]

[1] Department of Mathematics, Constantine the Philosopher University in Nitra, Tr. A. Hlinku 1, Nitra 94901, Slovakia
[2] Department of General Physics, I. N. Ulyanov Chuvash State University, Cheboksary 428015, Russia
[3] Department of Radio Engineering, I. N. Ulyanov Chuvash State University, Cheboksary 428015, Russia

* **Correspondence:** Email: vduris@ukf.sk; Tel: +421376408708.

Abstract: The relevance of the problem under study is due to the fact that the comparison is made for wavelets constructed in the time and frequency domains. The wavelets constructed in the time domain include all discrete wavelets, as well as continuous wavelets based on derivatives of the Gaussian function. This article discusses the possibility of implementing algorithms for multiscale analysis of one-dimensional and two-dimensional signals with the above-mentioned wavelets and wavelets constructed in the frequency domain. In contrast to the discrete wavelet transform (Mallat algorithm), the authors propose a multiscale analysis of images with a multiplicity of less than two in the frequency domain, that is, the scale change factor is less than 2. Despite the fact that the multiplicity of the analysis is less than 2, the signal can be represented as successive approximations, as with the use of discrete wavelet transform. Reducing the multiplicity allows you to increase the depth of decomposition, thereby increasing the accuracy of signal analysis and synthesis. At the same time, the number of decomposition levels is an order of magnitude higher compared to traditional multi-scale analysis, which is achieved by progressive scanning of the image, that is, the image is processed not by rows and columns, but by progressive scanning as a whole. The use of the fast Fourier transform reduces the conversion time by four orders of magnitude compared to direct numerical integration, and due to this, the decomposition and reconstruction time does not increase compared to the time of multiscale analysis using discrete wavelets.

Keywords: wavelet transform; decomposition; reconstruction; multiscale analysis; frequency response; digital filter

1. Introduction

Currently, Mallat algorithm is used for multiple-scale analysis (KMA) of signals, since he has developed a fast way to calculate discrete wavelet transform (WT). The idea of MSA is that the signal is decomposed according to the basis formed by shifts and multiple-scale copies of the wavelet function. KMA is an m-step discrete WT. The maximum value of m is called the depth of decomposition. In [1,2] the interpretation of the discrete WT is given. Sometimes discrete WT is used in conjunction with other transformations, for example, in [3]. In such cases, the disadvantages of discrete WT are still impossible to completely eliminate, because it is similar to how it is impossible to improve the error by calculating formulas with great accuracy if the measurements were made roughly. And the discrete WT has disadvantages:

1) The scaling factor changes only with a multiplicity of 2.

2) The wavelets are not symmetric or antisymmetric.

3) The accuracy of the calculation decreases with an increase in the decomposition level, since at each decomposition level the sample length decreases by 2 times.

4) The amplitude-frequency response of wavelets is uneven.

5) It is necessary to have a scaling function.

6) Progressive scan of the image is not used for multiple-scale analysis.

7) It is necessary to solve many equations for constructing wavelets of large orders.

To eliminate these disadvantages, the use of continuous WT is relevant. The difference between discrete and continuous WT is still in the method of calculation. If in order to calculate the wavelet coefficients of the next level with discrete WT, it is necessary to calculate the previous wavelet coefficients, then with continuous WT, all the wavelet coefficients can be calculated in parallel. At the hardware level, it can be imagined as if the signal passes through a parallel connection of filters. Continuous WT is calculated using computers, then this transformation is called a discrete version of continuous WT. In [4], such a transformation is called a discrete-time wavelet transform (DTWT).

It was noted in [5]: “For practice, it would be desirable to have orthogonal symmetric and asymmetric wavelets, but there are no such ideal wavelets”. Indeed, there are no orthogonal symmetric and antisymmetric wavelets for a WT. They write about continuous WT in [5]: “Coarse wavelets have a minimum of properties that wavelets should have, providing full-fledged capabilities in signal conversion technology: the analysis is not orthogonal; the possibility of reconstruction is not guaranteed; fast transformation algorithms and accurate reconstruction are impossible”.

The authors’ research shows that orthogonal symmetric and antisymmetric wavelets can be constructed, fast algorithms are possible, and the signal can be accurately reconstructed.

Wavelets and pulse characteristics of filters are closely interrelated. The wavelets with the largest scale factor are low-pass filters, those with the average scale factor are bandpass filters, and the smallest scale factor is high-pass filters. It can be said that the construction of orthogonal symmetric and antisymmetric wavelets is the same as the synthesis of digital filters with a rectangular amplitude-frequency response (frequency response). In the literature on digital filters, it is noted that rectangular frequency response leads to pulsations to the left and right of the cutoff frequency and the appearance of a transition band (Gibbs phenomenon). This is explained by the truncation of the Fourier series. The shorter the series, the greater the deviation of the frequency response from the initial one at steep drops. Explain the Gibbs phenomenon still using the convolution property.

In the theory of generalized Fourier transform (FT), it is proved that wavelets are orthogonal if the scalar product of these wavelets is zero. The authors’ research shows that the smaller the overlap

of the wavelet spectra for different scale coefficients, the smaller the scalar product of these wavelets. There will be no overlap when the spectra have a rectangular shape. For example, wavelets based on derivatives of the Gaussian function (coarse wavelets) have a smaller scalar product value if the order of the derivative is greater. The spectra of these wavelets are narrower, closer to a rectangular shape, there is less overlap and the reconstruction of the signal is more accurate. Although it is written about discrete wavelets that they are orthogonal, in fact this is not quite true, because the spectra of all such wavelets overlap. Just as continuous wavelets allow you to reconstruct a signal with one or another accuracy, so discrete wavelets allow you to reconstruct a signal with one or another accuracy and no better. But the continuous WT allows for multi-scale image analysis not only with a zoom factor equal to 2, but also with a multiplicity less than 2, to perform calculations in the frequency domain using the fast Fourier transform (FFT). The transition to the frequency domain allows us to design wavelets with specified properties that cannot be obtained in the time domain.

2. Research methods

During the research, it was possible to construct orthogonal symmetric and antisymmetric wavelets. Figure 1 shows one of these wavelets. Figure 2 shows the frequency response of this wavelet in decibels.

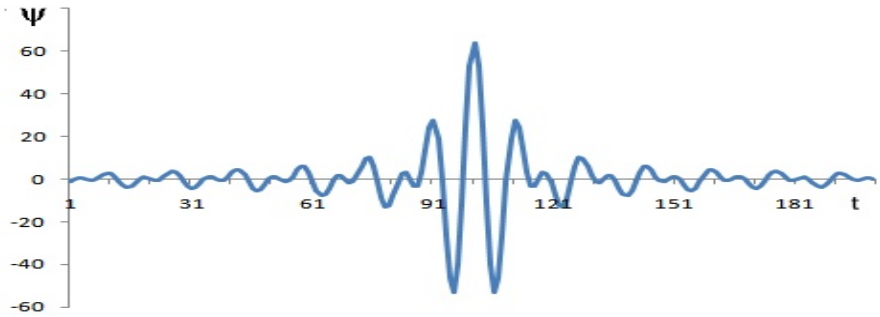

Figure 1. Orthogonal symmetric wavelet.

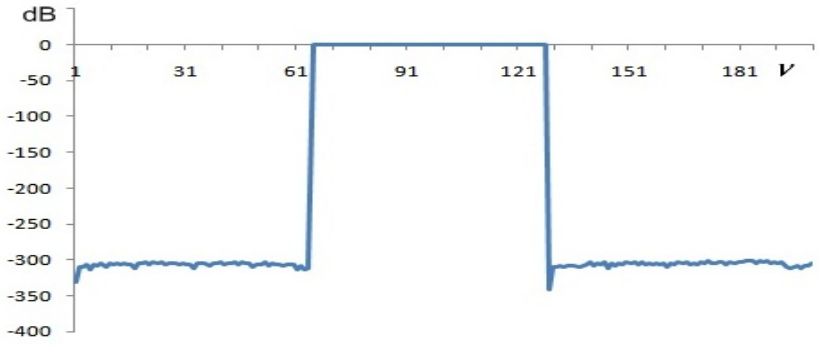

Figure 2. Frequency response of a symmetric orthogonal wavelet in dB.

It can be seen that the attenuation in the delay band is about -300 dB, which is comparable to the calculation error. The scalar product of such wavelets is zero within the margin of error. This is observed for all scalar products of wavelets with other scale coefficients. There are no ripples in the

bandwidth on the frequency response. Figure 3 shows the frequency response of this wavelet. It can be seen that there is no transition band. The covariance matrix for such a WT is diagonal. Figure 4 shows such a matrix. In Figure 5 covariance matrix for wavelets based on derivatives of the Gaussian function. Here the matrix is not diagonal, since the frequency response is not rectangular.

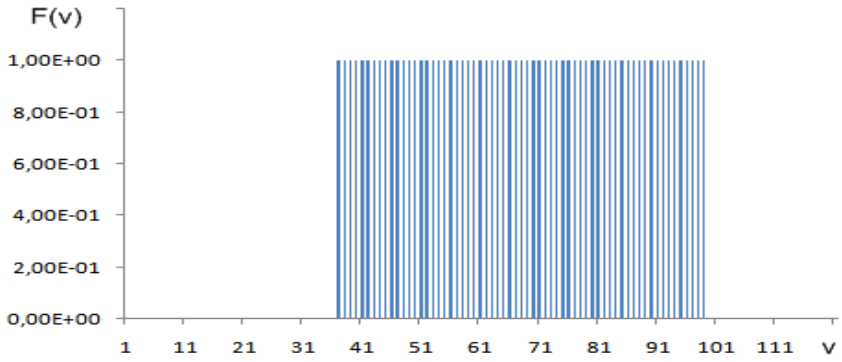

Figure 3. Frequency response of symmetric orthogonal wavelet.

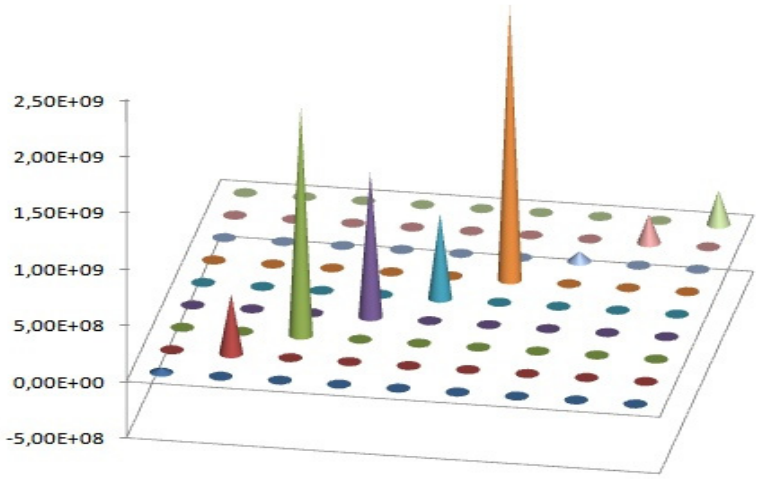

Figure 4. Covariance matrix of decomposition levels using wavelets constructed in the frequency domain.

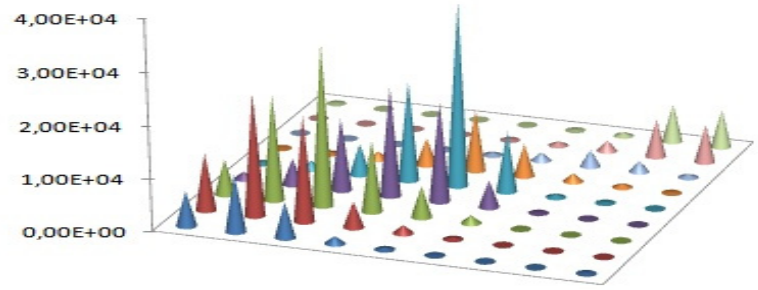

Figure 5. Covariance matrix of decomposition levels using wavelets constructed in the time domain.

If the covariance matrix has a diagonal form, then the wavelets of different decomposition levels are orthogonal. This is similar to the orthogonal Karhunen-Loève transformation, which leads the covariance matrix to a diagonal form. The diagonal matrix shows that the signal energy after the transformation is concentrated in a few significant wavelet coefficients of the transformation, that is, it is a prerequisite for signal compression. The main disadvantage of the Karhunen-Loève transform is that it is not universal, that is, different covariance matrices and, accordingly, different eigenfunctions are obtained for different types of signals. Also, there are no fast calculation algorithms for large matrices. Figure 6 shows the frequency response of the high-pass filter. The Gibbs phenomenon is clearly visible.

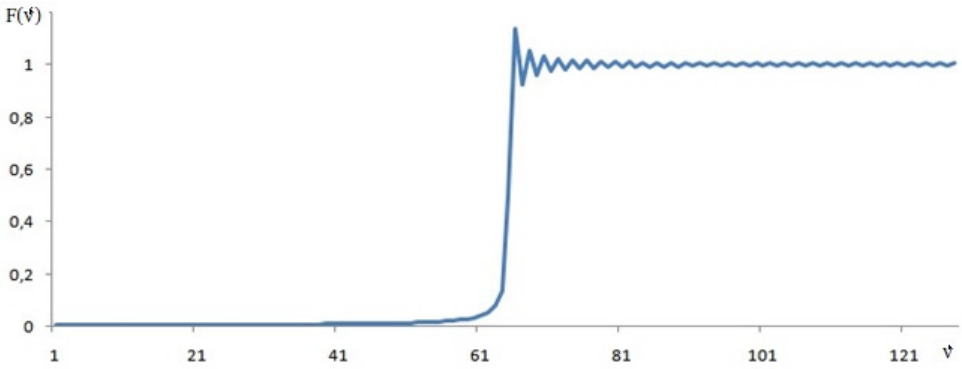

Figure 6. Frequency response of the high-pass filter.

Figure 7 shows the frequency response of high-pass filters synthesized in the time and frequency domains in decibels (logarithmic scale).

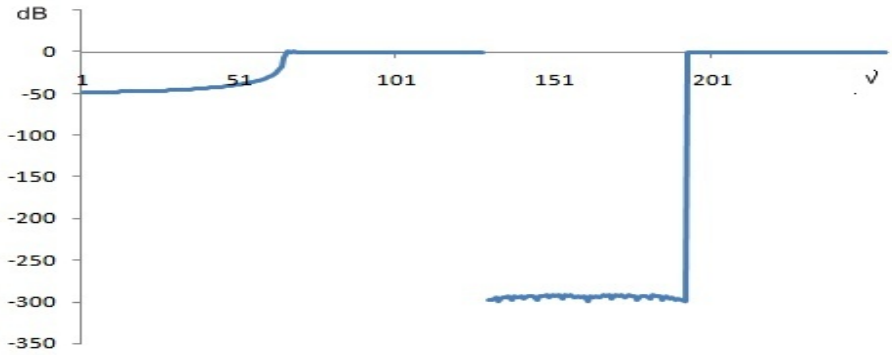

Figure 7. Frequency response of the high-pass filter synthesized in the time and frequency domains in decibels.

Up to a frequency of 128 units, the frequency response of the filter synthesized in the time domain is presented, and from 129 to 256–the filter synthesized in the frequency domain. The coefficients of the impulse response of the filter are calculated by the formula [6]:

$$b_{N+k} = \frac{1}{N+1} \sum_{j=\frac{N+1}{2}}^{N} \cos \frac{\pi k(j+0.5)}{N+1}$$

Figure 7 clearly shows how much the frequency characteristics of these filters differ when compared on the same scale. For a filter synthesized in the time domain, the Gibbs phenomenon is also observed. Figure 8 shows the frequency response with two band width in decibels. It can be said that the wavelets or digital filters obtained in the frequency domain have an ideal frequency response within the calculation error.

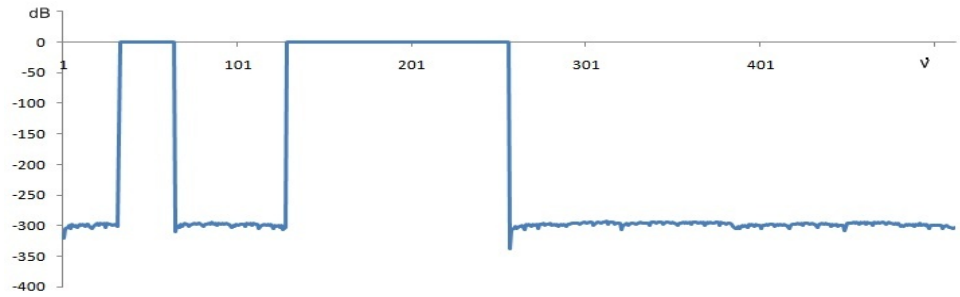

Figure 8. Frequency response of a filter with two passbands in decibels.

Algorithms for obtaining filters are presented in [7]. But filters are synthesized in the time domain, which leads to a transition band, and therefore a rectangular frequency response is not obtained.

3. Result

3.1. *Results of comparison of multiscale image analysis using the Mallat algorithm and the frequency domain algorithm*

Multiple-scale image analysis is possible not only with the use of the Mallat algorithm. Multiple-scale image analysis can be carried out both with wavelets based on derivatives of the Gaussian function and with wavelets constructed in the frequency domain, that is, decompose and reconstruct images. A correlation type measure was used to quantify the proximity between the reconstructed signal and the original signal. The calculated value of the Pearson correlation coefficient of the signal and the reconstructed signal was 0.999. The reconstructed images are no different from the original images and are better than for the Mallat algorithm.

The developed algorithms using FFT made it possible to reduce the calculation time of WT by four orders of magnitude compared to direct numerical integration:

$$W(a,b) = \frac{1}{\sqrt{a}} \int_{-\infty}^{\infty} S(t)\, \Psi\left(\frac{t-b}{a}\right) dt,$$

where a is the scale factor, b is the shift parameter. Algorithms for inverse and direct WT in the frequency domain are presented in [8,9].

Wavelets with rectangular frequency response made it possible to reduce the calculation time of direct WT in the frequency domain by 2 times compared to when wavelets based on derivatives of the Gaussian function were used. Like the inverse FT, there is an inverse continuous WT:

$$S(t) = C_{\Psi}^{-1} \int_{0}^{\infty} \int_{-\infty}^{\infty} \Psi\left(\frac{t-b}{a}\right) W(a,b) \frac{dadb}{a^{3+k}},$$

where C_{Ψ}–normalizing coefficient:

$$C_{\Psi} = \int_{-\infty}^{\infty} |F_{\Psi}(\omega)|^2 \cdot \omega^{-1} d\omega < \infty,$$

$F_{\Psi}(\omega)$–Fourier spectrum of the basis function, k–indicator of the degree of the scale multiplier.

Also, such wavelets made it possible to reduce the calculation time of the inverse WT signal with a sample size of 32,768 and 262,144 samples by 260 and 5000 times, respectively, compared with the FFT algorithm. The construction of symmetric and antisymmetric wavelets with a rectangular frequency response allowed the inverse WT to be calculated at least 10,000,000 times faster than with direct numerical integration. Profiling was carried out for a Celeron® processor with a frequency of 2.54 Ghz.

In contrast to the Mallat algorithm, the algorithm developed by the authors allows us to obtain a much larger number of decomposition levels, which allows us to study the image in more detail [3]. When using this algorithm, mosaicity does not appear when approximating the image. Figure 9(a) shows a 512 × 512 pixel color image reconstructed with the approximating coefficients of the fourth level for the algorithm in the frequency domain. In this case, a wavelet based on the Gaussian function of the 2nd order (MHAT-wavelet) is used.

(a) (b)

Figure 9. Reconstruction of the image with approximating coefficients of the fourth level: (a) the reconstructed image with the approximation coefficients of the fourth level for the algorithm in the frequency domain (b) the reconstructed image with the approximation coefficients of the fourth level for the Mallat algorithm.

Here, the scale factor a is 2 for comparison with the traditional Mallat transformation. For the developed algorithm, there is no need for approximating and detailing coefficients, there are only decomposition levels corresponding to the decomposition levels in the Mallat algorithm, and thus it becomes possible to compare the decomposition results. Figure 9(b) shows a reconstructed image with approximating coefficients of the fourth level. For the Mallat algorithm, a Daubechies db2 wavelet is used. The calculation was carried out using the MatLab application software package. In Figure 9(b) mosaicity is clearly visible. Image reconstruction with detailing coefficients also, when using the algorithm in the frequency domain, gives a clearer image than in the MatLab computer mathematics system (Mallat's algorithm). In Figure 10(a) a reconstructed image with the detailing coefficients of the first level for the algorithm in the frequency domain is presented. Figure 10(b) shows a reconstructed image with the detailing coefficients of the first level for the Mallat algorithm using the Daubechies wavelet (db2). Based on the developed algorithm in the frequency domain, in contrast to the discrete WT, it is possible to conduct multiscale image analysis with a multiplicity less than 2. This multi-scale analysis allows you to explore the image in a wide scale range, decomposing the image into dozens of levels. When moving from one level to another, the change in the image is visually barely noticeable. Figure 11 shows a multiscale image analysis with a multiplicity less than 2.

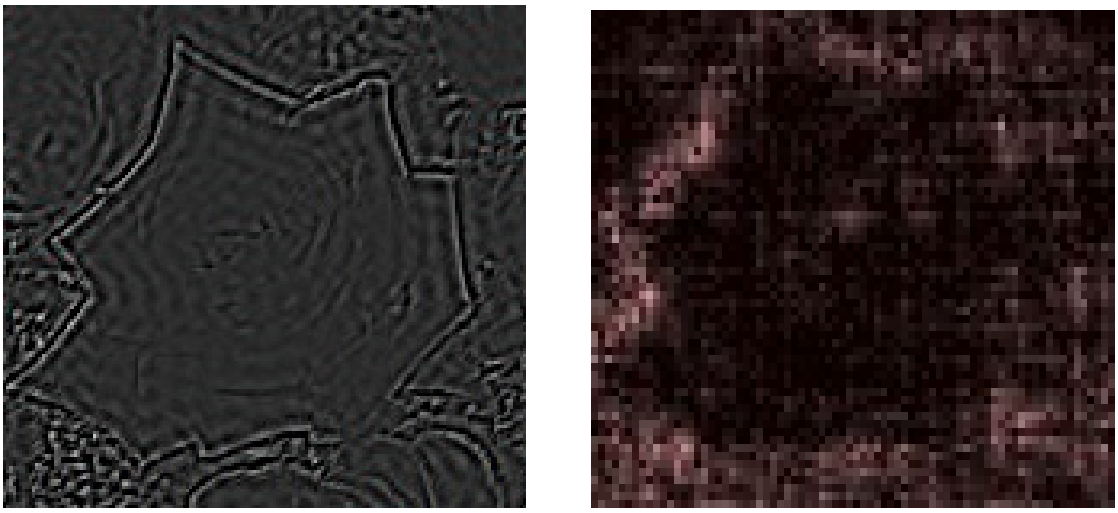

(a) (b)

Figure 10. Reconstruction of the image with detailing coefficients of the first level: (a) the reconstructed image with the detailing coefficients of the first level for the algorithm in the frequency domain, (b) the reconstructed image with the detailing coefficients of the first level for the Mallat algorithm.

(a) (b)

Figure 11. Multiscale image analysis with a multiplicity less than 2.

In Figure 11(a),(b), it is clearly noticeable that there are no colors at a small scale factor, the contour of the image stands out well. We also refer the reader to problematics of image edge detection based on singular value feature vector and gradient operator [10].

3.2. Results of comparison of the resolution of wavelets constructed in the time and frequency domains

Orthogonal symmetric and antisymmetric wavelets can also increase the spectral resolution.

Figure 12 shows the results of the wavelet transform of the sum of two sinusoids with frequencies slightly different from each other.

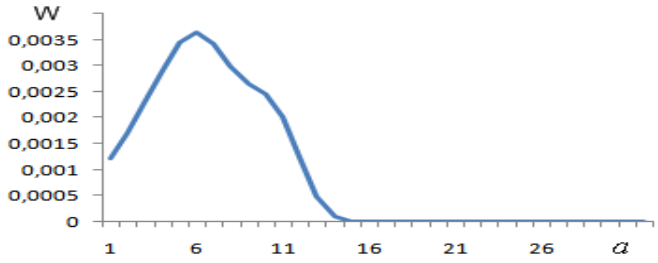

(a)

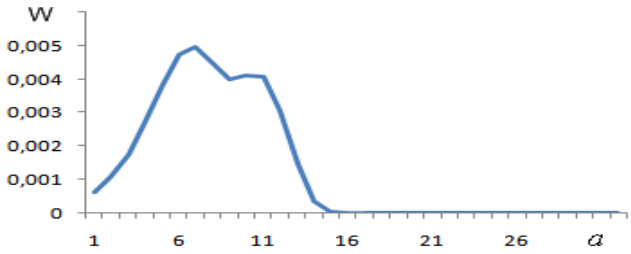

(b)

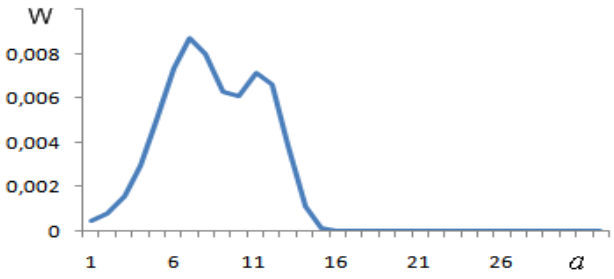

(c)

Figure 12. A slice of the wavelet transform with derivatives of the Gaussian function.

In Figure 12(a) uses the *MNAT* wavelet, that is, the second derivative of the Gaussian function, in Figure 12(b)–the third derivative of the Gaussian function, and in Figure 12(c)–the fourth derivative of the Gaussian function. For the fourth-order derivative of the Gaussian function, the resolution is better. Figure 13 shows the result of a wavelet transform of the same sum of sinusoids using an orthogonal symmetric wavelet constructed in the frequency domain.

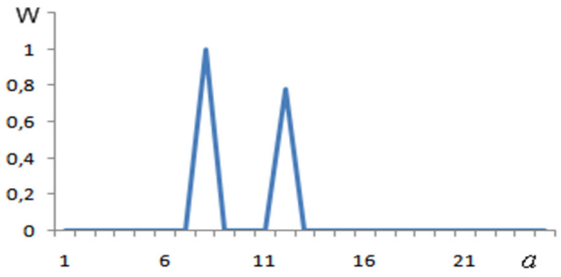

Figure 13. A slice of the wavelet transform based on an orthogonal symmetric wavelet.

The resolution of this wavelet is much higher than for wavelets based on derivatives of Gaussian functions. Figure 14 shows a slice of the wavelet transform for the sum of sinusoids with closer frequencies. For wavelets based on derivatives of the Gaussian function, these sinusoids are not resolved at all, that is, they are allocated as one sinusoid.

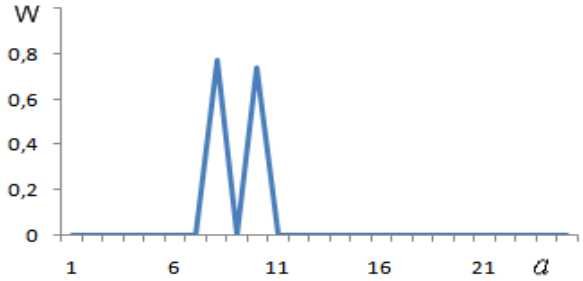

Figure 14. A slice of the wavelet transform based on an orthogonal symmetric wavelet.

4. Conclusions

Despite the fact that the conversion time using the Mallat algorithm is almost the same with the conversion time of the algorithm in the frequency domain, the image quality in the case of the implementation of the Mallat algorithm is much worse. When the wavelet order (dbN) is increased or other discrete wavelets are used, the mosaicity decreases, but the image quality remains significantly worse compared to the results when using wavelets based on derivatives of the Gaussian function and wavelets constructed in the frequency domain. Image reconstruction with detailing coefficients when using the algorithm in the frequency domain also gives a clearer image compared to the image obtained using the MatLab application software package. When reconstructing an image using all levels in MatLab, many colors are lost, when applying the algorithm in the frequency domain, the color gamut is preserved, the reconstructed image does not differ from the original.

The scientific literature does not present algorithms for multiscale analysis with a multiplicity less than 2. All papers describe signal processing based on discrete wavelet transform: papers [11–14] describe digital filter design sequence, papers [15–17] describe image processing. Among the papers using continuous wavelet transformation, we can note: [18] for processing seismic information, [19] for defect detection, [20] for signature verification, [21] for adaptive wavelet denoising, [22,23] for chemical analysis. In these papers, non-orthogonal wavelets are used and the transformation does not occur in the frequency domain, i.e., without the use of FFT. When compressing signals, noise

suppression, recognition and verification of objects, multi-scale analysis of signals in the time domain with a multiplicity equal to 2 is used. The use of multi-scale analysis in the frequency domain makes it possible to reconstruct the signal with greater accuracy. An increase in the number of decomposition levels means the use of bandpass filters with a reduced frequency range, which leads to more effective noise suppression. The construction of wavelets in the frequency domain allows us to obtain the maximum possible number of initial zero moments for a given sample. To obtain them in the time domain, it is necessary to solve a system with the same number of equations (more than 100). Obtaining wavelets with a large number of initial zero moments is the basis for the concentration of signal information in a few significant wavelet coefficients and thus serves as the basis for increasing the signal compression ratio.

MSA in the frequency domain is preferable compared to MSA in the time domain, since wavelets based on derivatives of the Gaussian function have a linear phase-frequency characteristic. In addition, wavelets constructed in the frequency domain have an ideal amplitude-frequency response. In this regard, the accuracy of signal reconstruction increases, that is, the transformation is truly orthogonal.

Conflict of interests

The authors declare no conflict of interest.

References

1. R. C. Guido, Effectively interpreting discrete wavelet transformed signals, *IEEE Signal Process. Mag.*, **34** (2017), 89–100. https://doi.org/10.1109/MSP.2017.2672759
2. R. C. Guido, Practical and useful tips on discrete wavelet transforms, *IEEE Signal Process. Mag.*, **32** (2015), 162–166. https://doi.org/10.1109/MSP.2014.2368586
3. Y. M. Li, D. Wei, L. Zhang, Double-encrypted watermarking algorithm based on cosine transform and fractional Fourier transform in invariant wavelet domain, *Inf. Sci.*, **551** (2021), 205–227. https://doi.org/10.1016/j.ins.2020.11.020
4. R. C. Guido, F. Pedroso, A. Furlan, R. C. Contreras, L. G. Caobianco, J. S. Neto, CWT × DWT × DTWT × SDTWT: Clarifying terminologies and roles of different types of wavelet transforms, *Int. J. Wavelets, Multiresolution Inf. Process.*, **18** (2020). https://doi.org/10.1142/S0219691320300017
5. O. S. Shumarova, S. A. Ignat'ev, Optimal choice of the type of wavelet for processing a signal from an eddy current sensor, *Vestn. SGTU*, **4** (2013), 128–132.
6. S. V. Umnyashkin, Theoretical foundations of digital signal processing and representation, In Russian, Moskow, FORUM: Infra-M Publ, (2009), 304.
7. D. Wei, Y. Li, Convolution and multichannel sampling for the offset linear canonical transform and their applications, *IEEE Trans. Signal Process.*, **67** (2019), 6009–6024. https://doi.org/10.1109/TSP.2019.2951191
8. V. Ďuriš, V. I. Semenov, S. G. Chumarov, Application of continuous fast wavelet transform for signal processing, London: Sciemcee Publishing, (2021), 181.
9. V. Ďuriš, S. G. Chumarov, G. M. Mikheev, K. G. Mikheev, V. I. Semenov, The orthogonal wavelets in the frequency domain used for the images filtering, *IEEE Access*, **8** (2020), 211125–211134. https://doi.org/10.1109/ACCESS.2020.3039373

10. J. Tang, Y. Wang, C. Huang, H. Liu, N. Al-Nabhan, Image edge detection based on singular value feature vector and gradient operator, *Math. Biosci. Eng.*, **17** (2020), 3721–3735. https://doi.org/10.3934/mbe.2020209
11. G. Qiu, W. Li, Y. Qi, W. Chen, A digital filtering algorithm based on four-channel wavelet and its application in active optical system, in *9th International Symposium on Advanced Optical Manufacturing and Testing Technologies: Optical Test, Measurement Technology, and Equipment*, 2019. https://doi.org/10.1117/12.2505100.
12. S. R. M. Penedo, M. L. Netto, J. F. Justo, Designing digital filter banks using wavelets, *EURASIP J. Adv. Signal Process.*, **33** (2019). https://doi.org/10.1186/s13634-019-0632-6
13. R. I. Umamaheswar, Discrete wavelet transforms using daubechies wavelet, *IETE J. Res.*, **47** (2001), 169–171. https://doi.org/10.1080/03772063.2001.11416221
14. S. Gyanendra, S. R. Chiluveru, B. Raman, M. Tripathy, B. K. Kaushik, Memory efficient architecture for lifting-based discrete wavelet packet transform, *IEEE Trans. Circuits Syst. II: Express Briefs*, **68** (2021), 1373–1377. https://doi.org/10.1109/TCSII.2020.3028092
15. E. J. Stollnitz, T. D. Derose, D. H. Salesin, Wavelets for computer graphics: A primer, USA, University of Washington, 1994.
16. P. Singh, Wavelet transform in image processing: Denoising, segmentation and compression of digital, images, *Int. J. Sci. Res. Sci., Eng. Technol.*, **2** (2016), 1137–1140.
17. M. M. Ameen, A. Eleyan, G. Eleyan, Wavelet transform based face recognition using SURF descriptors, *Int. J. Electron. Electr. Eng.*, **5** (2017), 94–98. https://doi.org/10.18178/ijeee.5.1.94-98
18. M. T. Naseer, S. Asim, Application of instantaneous spectral analysis and acoustic impedance wedge modeling for imaging the thin beds and fluids of fluvial sand systems of Indus Basin, Pakistan, *J. Earth Syst. Sci.*, **127** (2018), 1–20. https://doi.org/0.1007/s12040-018-0997-1
19. Z. Liu, H. Chen, K. Sun, C. He, B. Wu, Full non-contact laser-based Lamb waves phased array inspection of aluminum plate, *J. Visualization*, **21** (2018), 751–761. https://doi.org/10.1007/s12650-018-0497-z
20. O. Alpar, Online signature verification by continuous wavelet transformation of speed signals, *Expert Syst. Appl.*, **104** (2018), 33–42. https://doi.org/10.1016/j.eswa.2018.03.023.
21. X. Xu, M. Luo, Z. Tan, R. Pei, Echo signal extraction method of laser radar based on improved singular value decomposition and wavelet threshold denoising, *Infrared Phys. Technol.*, **92** (2018), 327–335. https://doi.org/10.1016/j.infrared.2018.06.028
22. D. Li, T. Cheng, M. Jia, K. Zhou, N. Lu, X. Yao, et al., PROCWT: Coupling PROSPECT with continuous wavelet transform to improve the retrieval of foliar chemistry from leaf bidirectional reflectance spectra, *Remote Sens. Environ.*, **206** (2018), 1–14. https://doi.org/10.1016/j.rse.2017.12.013
23. A. Yadav, N. Sengar, A. Issac, M. K. Dutta, Image processing based acrylamide detection from fried potato chip images using continuous wavelet transform, *Comput. Electron. Agric.*, **145** (2018), 349–362. https://doi.org/10.1016/j.compag.2018.01.012